



UNIVERSITÀ  
DEGLI STUDI  
FIRENZE

## FLORE

# Repository istituzionale dell'Università degli Studi di Firenze

### **The crystal structure of parkinsonite, nominally $\text{Pb}_7\text{MoO}_9\text{Cl}_2$ : a naturally occurring Aurivillius phase**

Questa è la Versione finale referata (Post print/Accepted manuscript) della seguente pubblicazione:

*Original Citation:*

The crystal structure of parkinsonite, nominally  $\text{Pb}_7\text{MoO}_9\text{Cl}_2$ : a naturally occurring Aurivillius phase / G.O. Lepore; M. D. Welch. - In: MINERALOGICAL MAGAZINE. - ISSN 0026-461X. - STAMPA. - 74:(2010), pp. 269-275. [10.1180/minmag.2010.074.2.269]

*Availability:*

The webpage <https://hdl.handle.net/2158/956740> of the repository was last updated on

*Published version:*

DOI: 10.1180/minmag.2010.074.2.269

*Terms of use:*

Open Access

La pubblicazione è resa disponibile sotto le norme e i termini della licenza di deposito, secondo quanto stabilito dalla Policy per l'accesso aperto dell'Università degli Studi di Firenze (<https://www.sba.unifi.it/upload/policy-oa-2016-1.pdf>)

*Publisher copyright claim:*

La data sopra indicata si riferisce all'ultimo aggiornamento della scheda del Repository FloRe - The above-mentioned date refers to the last update of the record in the Institutional Repository FloRe

(Article begins on next page)

# The crystal structure of parkinsonite, nominally $\text{Pb}_7\text{MoO}_9\text{Cl}_2$ : a naturally occurring Aurivillius phase

G. O. LEPORE<sup>1</sup> AND M. D. WELCH<sup>2</sup>

<sup>1</sup> Dipartimento di Scienze della Terra, Università di Firenze, Firenze, Italy

<sup>2</sup> Department of Mineralogy, The Natural History Museum, Cromwell Road, London SW7 5BD, UK

[Received 19 March 2010; Accepted 26 April 2010]

## ABSTRACT

The crystal structure of the sheet oxychloride mineral parkinsonite, nominally  $\text{Pb}_7\text{MoO}_9\text{Cl}_2$ , has been determined for synthetic and natural crystals of analysed compositions,  $(\text{Pb}_{7.28}\text{Mo}_{0.72})\text{O}_{8.96}\text{Cl}_{1.96}$  and  $(\text{Pb}_{7.23}\text{Mo}_{0.40}\text{V}_{0.37})\text{O}_{8.90}\text{Cl}_{1.82}$ , respectively. Parkinsonite is tetragonal, space group  $I4/mmm$ . Unit-cell parameters for synthetic and natural crystals are:  $a_{\text{synthetic}} = 3.9773(4) \text{ \AA}$ ,  $c_{\text{synthetic}} = 22.718(4) \text{ \AA}$ ,  $V_{\text{synthetic}} = 359.38(5) \text{ \AA}^3$ , and  $a_{\text{natural}} = 3.9570(3) \text{ \AA}$ ,  $c_{\text{natural}} = 22.634(5) \text{ \AA}$ ,  $V_{\text{natural}} = 354.40(5) \text{ \AA}^3$ . Final agreement indices ( $R_1$ ,  $wR_2$ ) for refinements of the two crystals are 0.024, 0.067 (synthetic) and 0.036, 0.078 (natural). Although a superlattice has been identified by electron diffraction for crystals of both samples (Welch *et al.*, 1996), only the substructure could be determined by X-ray diffraction. This X-ray invisibility of the superstructure has also been observed for the closely related sheet oxychlorides asisite and schwartzembergite, for both of which superstructure motifs have been identified by electron diffraction. The Pb(1) site of both parkinsonite crystals is fully occupied by Pb. Refinement of the Pb content of the Pb(2) site for the synthetic and natural crystals gives occupancies of 0.85(1) and 0.70(1) respectively, corresponding to 3.40 and 2.80 Pb(2) a.p.f.u. respectively. The substituent cation Mo (synthetic crystal) and [Mo+V] (natural crystal) was located at a distance of 0.5 Å from Pb(2), being displaced along the fourfold axis. The reduced occupancy of Pb(2) is due to substitution by Mo or [Mo+V]. No evidence for separate Mo and V sites in the substructure of natural parkinsonite was found. Refined occupancies of the Cl site are 0.84(4) and 0.91(5) for the synthetic and natural crystals, respectively, and are consistent with the 9:1 superstructure component identified by electron diffraction.

**KEYWORDS:** parkinsonite, crystal structure, Aurivillius phase.

## Introduction

ABOUT a dozen naturally occurring Aurivillius-type minerals have been reported, in which the elements substituting for  $\text{Pb}^{2+}$  include B, C, Si,  $\text{As}^{3+}$ ,  $\text{As}^{5+}$ ,  $\text{Sb}^{3+}$ ,  $\text{Sb}^{5+}$ ,  $\text{Mo}^{6+}$ ,  $\text{W}^{6+}$ ,  $\text{I}^{3+}$  and  $\text{I}^{5+}$ . Two major types of structural topology can be recognized in the Pb sheet oxychlorides that relate to the way in which the substituent cation is embedded into the PbO sheet, as we now describe.

## Group I structures

In members of this group the substituent cation is embedded as a tetrahedral or triangular oxyanion ( $\text{SO}_4^{2-}$ ,  $\text{VO}_4^{3-}$ ,  $\text{BO}_3^{3-}$ ,  $\text{CO}_3^{2-}$ ) with major local restructuring of the PbO sheet, including the creation of vacancies at O sites. Examples of such structures include kombatite ( $\text{VO}_4^{3-}$ : Cooper and Hawthorne, 1994), symesite ( $\text{SO}_4^{2-}$ : Welch *et al.*, 2000), sahlinite ( $\text{AsO}_4^{3-}$ : Bonaccorsi and Pasero, 2003), and mereheadite ( $\text{BO}_3^{3-}$ ,  $\text{CO}_3^{2-}$ : Krivovichev *et al.* 2009). Asisite, nominally  $\text{Pb}_7\text{SiO}_8\text{Cl}_2$  (Rouse *et al.*, 1988; Welch, 2004), presumably has Si present as tetrahedral  $\text{SiO}_4$  groups, although the ordered superstructure has not been determined.

\* E-mail: mdw@nhm.ac.uk

DOI: 10.1180/minmag.2010.074.2.269

## Group II structures

In this group, the substituent species replaces  $\text{Pb}^{2+}$  apparently with minimal changes in the  $\text{PbO}$  sheet and no disruption of the O array; no O vacancies are created, although additional O atoms can occur between adjacent  $\text{PbO}$  sheets to charge-balance and complete the coordination of substituent atom as, for example, the square-pyramidal  $\text{WO}_5$  group in pinalite  $\text{Pb}_3\text{WO}_5\text{Cl}_2$  (Grice and Dunn, 2000) and synthetic pinalite derivatives (Charkin and Lightfoot, 2006).

In addition to structural changes at the cation sites, there is considerable variation in the types of linkages formed between adjacent  $\text{PbO}$  sheets, which include: bridging  $\text{H}_2\text{O}$  groups (symesite),  $\text{Pb}-\text{Cl}-\text{Pb}$  bridges (pinalite/seeligerite),  $\text{M}^{n+}-\text{O}-\text{Pb}$  bridges (pinalite) and, uniquely in mereheadite, additional  $\text{PbCl}$  interlayer groups.

The different modes of embedding the substituent cation into the  $\text{PbO}$  sheet have important effects upon diffraction behaviour. For Group II structures, in which there is minimal disruption of the  $\text{PbO}$  sheet, only the tetragonal  $I4/mmm$  substructure is found by single-crystal X-ray diffraction (XRD). However, superlattices (supersheet motifs) have been recognized by electron diffraction (TEM) for parkinsonite (Welch *et al.*, 1996) and schwartzembergite (Welch *et al.*, 2001). By contrast, the full superstructures of Group-I phases are readily identified by X-ray diffraction, due to the highly visible superlattice reflections. Evidently, the major modifications of the  $\text{PbO}$  sheets of Group I structures lead to identifiable and significant effects upon diffraction patterns. There is, however, one exception: asisite, nominally  $\text{Pb}_7\text{SiO}_8\text{Cl}_2$  (Rouse *et al.*, 1988), for which only a substructure has been determined by X-ray diffraction, despite clear evidence from electron diffraction of a well developed superstructure based upon a  $\text{Pb}_{12}\text{Si}$  ordering stoichiometry (Welch, 2004). Attempts to locate the superlattice reflections of asisite using CCD area detectors have been unsuccessful. Presumably, the Si in asisite is tetrahedrally coordinated, and so it is expected that the mineral has a Group-I structure type, and so the inability of X-ray diffraction to register superlattice reflections is surprising.

Parkinsonite was described as a new mineral species by Symes *et al.* (1994), who reported a general formula  $(\text{Pb}, \text{Mo}, \square)_8\text{O}_8\text{Cl}_2$  ( $Z = 1$ ) which implies the presence of vacancies at cation sites.

On the basis of close similarities with the X-ray powder diffraction patterns of known synthetic phases (Aurivillius, 1982), they inferred that parkinsonite was an Aurivillius phase. No single-crystal structure determination of parkinsonite has been made to date largely due to the scarcity of suitable natural material. The unit cell reported by Symes *et al.* (1994) corresponds to one of the subcells ( $4 \text{ \AA} \times 4 \text{ \AA} \times 23 \text{ \AA}$ ) that is characteristic of the  $\text{PbO}$ -based sheet oxychlorides, and also occurs in asisite (Rouse *et al.*, 1988; Welch, 2004).

Welch *et al.* (1996) studied natural and synthetic parkinsonites by electron diffraction (TEM) and recognized a superlattice based on a  $8.95 \text{ \AA} \times 8.95 \text{ \AA} \times 23 \text{ \AA}$  motif. This motif suggests a 10-site ordering scheme with  $\text{Pb}_9\text{Mo}$  cation stoichiometry and a formula  $(\text{Pb}_9\text{Mo})\text{O}_{11}\text{Cl}_2$  ( $Z = 5$ ). Electron microprobe analyses of synthetic parkinsonites synthesized from different bulk compositions converge upon this  $\text{Pb}:\text{Mo}$  ratio (Welch *et al.*, 1996), indicating that a 9:1 superstructure is a significant component of the structures of these phases. Recasting this formula in terms of subcell content gives  $\text{Pb}_{7.2}\text{Mo}_{0.8}\text{O}_{8.8}\text{Cl}_{1.6}$  ( $Z = 1$ ): the Cl content of the supercell is reduced by 20% relative to the nominal formula  $\text{Pb}_7\text{MoO}_9\text{Cl}_2$ . Hence, the presence of this superstructure should be registered compositionally and by reduced occupancy of the Cl site in the average  $I4/mmm$  substructure. Here, we report the first full structure determination of parkinsonite from single-crystal XRD experiments on natural and synthetic crystals.

## Experimental methods

### Electron microprobe analysis

After the XRD experiment (described below), the two crystals were mounted on a glass slide, carbon coated and analysed by wavelength-dispersive electron microprobe analysis (WDS) using a Cameca microprobe operated at 25 kV and 10 nA, with a  $2 \text{ \mu m}$  final beam diameter. Calibration standards used were synthetic  $\text{Pb}_5(\text{VO}_4)_3\text{Cl}$  (for  $\text{Pb}-M\alpha$ ,  $\text{V}-K\alpha$ ,  $\text{Cl}-K\alpha$ ), GaAs (for  $\text{As}-L\alpha$ ) and Mo metal (for  $\text{Mo}-L\alpha$ ). Electron microprobe analyses give average empirical formulae  $\text{Pb}_{7.28(1)}\text{Mo}_{0.72(1)}\text{O}_{8.96}\text{Cl}_{1.96(2)}$  (synthetic, 12 analyses) and  $\text{Pb}_{7.24(0)}\text{Mo}_{0.40(1)}\text{V}_{0.37(1)}\text{O}_{8.90}\text{Cl}_{1.82(3)}$  (natural, 19 analyses) – in good agreement with the compositions determined by Welch *et al.* (1996).

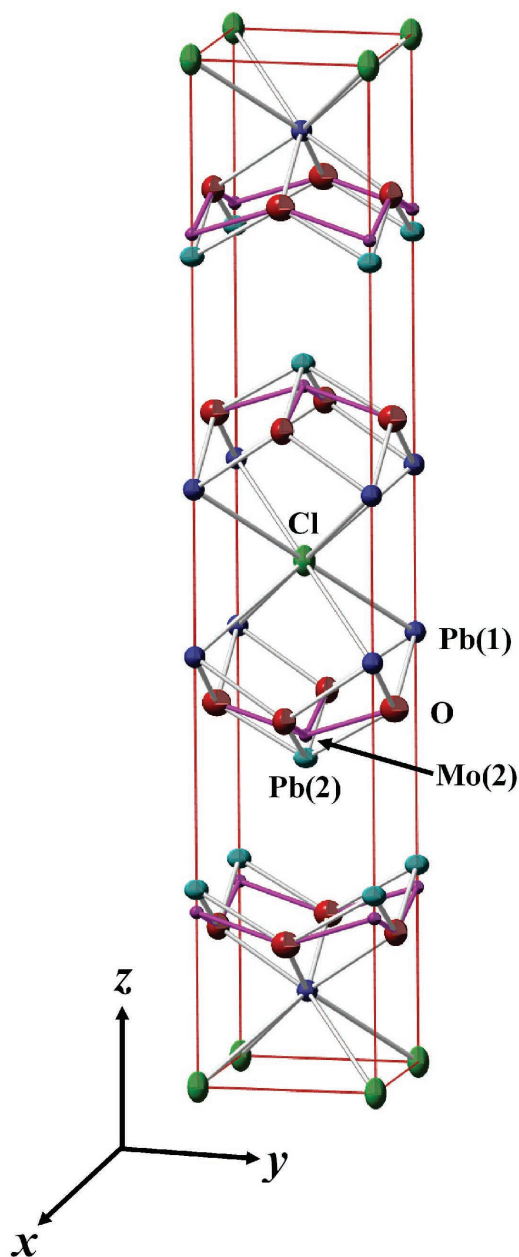


FIG. 1. The crystal structure of synthetic parkinsonite. Anisotropic displacement ellipsoids of Pb, O and Cl are shown at the 50% level. The displacement volume of Mo (refined isotropically) is shown as a sphere at the 50% level. The Mo–O bond is shown in purple. The separation between Mo(2) and Pb(2) is 0.5 Å.

#### X-ray diffraction studies

Thin, platy crystals of natural and synthetic parkinsonite were attached to a 0.01 mm diameter non-diffracting carbon fibre and mounted on an Enraf Nonius Turbo-CAD4 diffractometer. Crystals were selected on the basis of optical and diffraction quality. Unit-cell parameters (Table 1) were obtained from the setting angles of 25 reflections in the range  $3^\circ < \theta < 19^\circ$ , by four-position centring (SET4 option on the CAD4). A whole sphere of intensity data was collected for  $3^\circ < \theta < 30^\circ$  using  $\omega$ - $2\theta$  scans, with scan speeds inversely proportional to intensity as measured by prescans. Data reduction, structure solution (SHELXS: Sheldrick, 2008) and refinement (SHELXL: Sheldrick, 2008) were carried out within the WinGX program suite (Farrugia, 1999). Reflections were corrected for Lorentz-polarization and background effects. A Gaussian absorption correction based on face-indexing was then applied. Merging statistics, obtained using SORTAV (Blessing, 1987), were consistent with point group  $4/mmm$ , for which redundancy-independent  $R_{\text{int}}$  values of 0.038 (natural) and 0.035 (synthetic) were obtained. Absorption-corrected intensities were reduced to  $F^2$ . Details relating to data collection and structure refinement are summarized in Table 1.

In their electron-diffraction (TEM) study of natural and synthetic parkinsonites from the same samples as those studied here, Welch *et al.* (1996) recognized a superlattice based upon an  $a = 8.95$  Å tetragonal motif ( $Z = 5$ ), which they attributed to ordering on a  $\text{Pb}_9\text{Mo}$  scheme. The superlattice reflections at  $\frac{1}{3} [130]^*$  recorded by electron diffraction were much weaker than the sublattice reflections ( $h + k + l = 2n$ ). We attempted to collect these superlattice reflections for the natural crystal for both possible twinned superlattice orientations reported by Welch *et al.* (1996), but no detectable diffracted intensity was recorded after 10 min for five low-angle superlattice reflections ( $< 10^\circ\theta$ ). We also attempted to find the weak superlattice reflections by checking using a CCD area detector, but none were registered (M.A. Cooper, pers. comm. to MDW). Welch *et al.* (1996) also reported that weak superlattice reflections were only registered by precession photography using a high-sensitivity film and an exposure time of 4 d.

In their study of the closely-related mineral schwartzembergite,  $\text{Pb}_5\text{I}^{3+}\text{O}_6\text{H}_2\text{Cl}_3$ , Welch *et al.* (2001) reported that, while XRD identifies only a

TABLE 1. Experimental details relating to the data collection, data reduction and structure refinement of synthetic and natural parkinsonites of this study.

	Synthetic	Natural
Empirical formula (Pb + Mo + V = 8)*	Pb <sub>7.28</sub> Mo <sub>0.72</sub> O <sub>8.96</sub> Cl <sub>1.96</sub>	Pb <sub>7.23</sub> Mo <sub>0.40</sub> V <sub>0.37</sub> O <sub>8.90</sub> Cl <sub>1.82</sub>
Temperature (K)	298	298
Wavelength (Å)	0.71073	0.71073
Crystal system	Tetragonal	Tetragonal
Space group	<i>I4/mmm</i>	<i>I4/mmm</i>
Unit-cell dimensions (Å)	<i>a</i> = 3.9773 (4) <i>c</i> = 22.718 (4)	<i>a</i> = 3.9570 (3) <i>c</i> = 22.634 (5)
Unit-cell volume (Å <sup>3</sup> )	359.38(5)	354.40(5)
<i>Z</i>	1	1
Density (calculated) (g cm <sup>-3</sup> )	8.060	8.167
Absorption coefficient (mm <sup>-1</sup> )	82.9	84.1
Crystal size (mm)	0.150 × 0.108 × 0.010	0.116 × 0.100 × 0.012
$\theta$ range for data collection	3.6–29.7°	3.6–29.9°
<i>h</i> , <i>k</i> , <i>l</i> ranges	±5, ±5, ±31	±5, ±5, ±31
Reflections collected	2096	2096
Unique reflections, <i>R</i> <sub>int</sub>	198, 0.035	198, 0.038
Reflections <i>I</i> > 2σ( <i>I</i> )	195	194
Data completeness to $\theta_{\max}$	99.5% ( $\theta_{\max}$ = 29.7°)	99.5% ( $\theta_{\max}$ = 29.9°)
Absorption correction	Gaussian	Gaussian
Max./min. transmission	0.3129/0.0114	0.3095/0.0216
Refinement method	Full-matrix least-squares on <i>F</i> <sup>2</sup>	Full-matrix least-squares on <i>F</i> <sup>2</sup>
Weighting coefficients <i>a</i> , <i>b</i> **	0.0293, 10.27	0.0339, 4.53
Extinction coefficient	0.0063(6)	—
Data/restraints/parameters	198/0/17	198/0/16
<i>R</i> <sub>1</sub> [ <i>F</i> > 4σ( <i>F</i> )], <i>R</i> <sub>1</sub> all, <i>wR</i> <sub>2</sub> all	0.024, 0.025, 0.067	0.036, 0.037, 0.078
GoF on <i>F</i> <sup>2</sup>	1.20	1.22
Largest diff. peak and hole (e Å <sup>-3</sup> )	2.0 and -2.8	1.2 and -0.4

\* Oxygen content calculated for charge balance

\*\* Weight = 1/[σ<sup>2</sup>(*F*<sub>o</sub><sup>2</sup>) + (*aP*)<sup>2</sup> + *bP*] where *P* = (max(*F*<sub>o</sub><sup>2</sup>, 0) + 2*F*<sub>c</sub><sup>2</sup>)/3

$$R_{\text{int}} = (n/n - 1)^{1/2} [F_o^2 - F_o(\text{mean})^2] / \Sigma F_o^2 \quad R_1 = \Sigma ||F_o| - |F_c|| / \Sigma |F_o|$$

$$\text{GoF} = \{\Sigma [w(F_o^2 - F_c^2)^2] / (n - p)\}^{1/2} \quad wR_2 = \{\Sigma [w(F_o^2 - F_c^2)^2] / \Sigma [w(F_o^2)^2]\}^{1/2}$$

tetragonal *I4/mmm* substructure, the mineral is optically biaxial, an observation originally made by Smith and Prior (1911) who determined 2*V* = 38°. Evidently, for these minerals, optical character is sensitive to the superstructure. We obtained interference figures for both crystals of parkinsonite and found that they were uniaxial, implying that the superstructure is also likely to be tetragonal (*I4/m*), as proposed by Welch *et al.* (1996). Consequently, we determined the tetragonal *I4/mmm* substructures for the two crystals studied here.

## Results

### Structure solution and refinement

Neutral scattering factors were used for Pb, Mo, Cl and O atoms. Structure solution located the two non-equivalent Pb atoms and the Cl atom of the subcell. *E*-statistics imply that the crystals are centrosymmetric. Refinement of the structures of both crystals was carried out in space group *I4/mmm*. The O atom appeared in the first difference-Fourier synthesis of isotropic refinement, as did a significant electron density maximum of 10–12 e.Å<sup>-3</sup> at ~0.5 Å from

Pb(2). This maximum appears early in the refinements of both crystals. Considering the substructure of schwartzembergite (Welch *et al.*, 2001), in which the substituent  $\text{I}^{3+}$  cation occurs at  $\sim 0.6$  Å from the Pb(2) atom, we assigned this peak to substituent Mo. We observed that  $U_{\text{iso}}$  values of Pb(2) in both structures were initially about twice those of Pb(1), e.g. for the synthetic crystal at this stage of the refinement,  $U_{\text{iso}}$  of Pb(1) was  $0.017 \text{ \AA}^2$  and  $U_{\text{iso}}$  of Pb(2) was  $0.035 \text{ \AA}^2$ . This observation is consistent with partial occupancy of Pb(2), most likely corresponding to replacement by the lighter scatterer Mo. In order to avoid problems with strong correlations between Pb(2) site occupancy and  $U_{\text{iso}}$ , and to get a reasonable estimate of the level of partial occupancy of Pb(2), a single  $U_{\text{iso}}$  was refined initially for both Pb atoms. This approach led to stable refinement and sensible Pb(2) occupancies and  $U_{\text{iso}}$  values for both crystals: Pb(2) site occupancies are 0.85(1) and 0.70(1) for synthetic and natural crystals respectively. An attempt was made to refine the occupancy of the Mo(2) and Pb(2) sites simultaneously, but this led to unstable refinement, presumably due to the small Mo content and resulting weak scattering from the Mo(2) site compared with that of the adjacent Pb(2) site 0.5 Å distant. Consequently, occupancy of Pb(2) for each crystal was fixed at its refined value (see above) and the missing occupancy assigned to Mo, which was then also fixed. In assigning the Mo occupancy as  $[1 - \text{occ Pb(2)}]$ , we assume that there are no vacancies, i.e.  $[\text{occ Pb(2)} + \text{occ Mo(2)}] = 1$ . As all related Pb sheet-oxychlorides in which there is partial substitution of Pb do not have cation vacancies, we consider that this assumption is justified. After fixing the Pb(2) occupancy [and thereby also that of Mo(2)], the Pb(1) and Pb(2) were uncoupled and  $U_{\text{iso}}$  was refined for each, leading to comparable values of  $\sim 0.025 \text{ \AA}^2$ . This procedure was used successfully in the refinement of the substructure of asisite (Welch, 2004).

Electron microprobe analysis of the natural parkinsonite crystal shows the presence of  $0.37 \text{ V}^{5+}$  a.p.f.u. in addition to  $0.40 \text{ Mo}^{6+}$  a.p.f.u. The  $\text{V}^{5+}$  substitutes for  $\text{Pb}^{2+}$  in komatite (Cooper and Hawthorne, 1994) in which it forms a tetrahedral  $\text{VO}_4$  group. As only a single clear residual maximum was observed in the difference-Fourier map (see above), we infer that separate Mo and V sites are not distinguished in the substructure of natural parkinsonite. Nonetheless, we attempted to model mixed occupancy at the

Mo(2) site of natural parkinsonite based upon a fixed occupancy of  $0.1\text{Mo} + 0.1\text{V}$  [there are four Mo(2) sites per unit cell] indicated by electron microprobe analysis; the Pb(2) site was then also fixed at 0.8 Pb. However, such refinements were unstable and gave unreasonable occupancies and an implausibly large  $U_{\text{iso}}$ . We point out that the difference in scattering power for the Mo(2) site when it is occupied by  $0.1 \text{ Mo} + 0.1 \text{ V}$  (6.5 e) is very similar to that when occupied only by  $0.2 \text{ Mo}$  (8.4 e). Consequently, we settled for a Mo-only refinement of Mo(2) in natural parkinsonite, as this led to stable refinement and reasonable values for occupancy and  $U_{\text{iso}}$ .

At this point in the refinement, we also checked for partial occupancy of the Cl site, in view of the  $(\text{Pb}_9\text{Mo})\text{O}_{11}\text{Cl}_2$  superstructure identified by Welch *et al.* (1996) using electron diffraction, which implies 80% occupancy of the Cl site in the subcell. Refined fractional occupancies of Cl for the synthetic and natural crystals are 0.84(4) and 0.91(5), respectively. Thus, a reduced Cl occupancy is indicated that is consistent with the presence of the  $(\text{Pb}_9\text{Mo})\text{O}_{11}\text{Cl}_2$  superstructure. After a further six cycles of isotropic refinement, Pb, Cl and O atoms were refined anisotropically. Molybdenum was refined isotropically throughout for both structures.

Weighting based upon reflection intensity was used in the last stages of refinement and finally an extinction correction, suggested by *SHELX*, was employed for synthetic parkinsonite. No extinction correction was indicated by *SHELX* for the natural crystal. Looking at the differences between observed and calculated structure factors for the two crystals, we found that there is a systematically greater discrepancy for the synthetic crystal compared with the natural, which is consistent with applying an extinction correction to the former. Furthermore, the synthetic crystal appears to be of a better quality than the natural (an almost perfect cleavage and sharper, narrower diffraction maxima). We point out that, while an extinction correction for the synthetic crystal improved the final result of the refinement, the refined structures for the two crystals are very similar. Experimental details are summarized in Table 1, and atom coordinates and displacement parameters are given in Table 2. Tables of structure factors for the two crystals are lodged with the Principal Editor of *Mineralogical Magazine* and are available from [http://www.minersoc.org/pages/e\\_journals/dep\\_mat\\_mm.html](http://www.minersoc.org/pages/e_journals/dep_mat_mm.html). The crystal structure is shown in Fig. 1.



TABLE 2. Atom coordinates and anisotropic displacement parameters ( $\text{\AA}^2$ ) for synthetic (upper) and natural (lower) parkinsonites of this study.

Atom	<i>z</i>	Occupancy	<i>U</i> <sub>11</sub>	<i>U</i> <sub>22</sub>	<i>U</i> <sub>33</sub>	<i>U</i> <sub>eq</sub>
Pb(1)	0.41846(3)	1	0.02045(3)	0.02045(3)	0.0224(4)	0.0211(3)
	0.41822(3)	1	0.0166(3)	0.0166(3)	0.0170(4)	0.0167(3)
Pb(2)	0.19188(5)	0.85 (1) *	0.0272(4)	0.0272(4)	0.0185(5)	0.0243(3)
	0.19446(7)	0.70 (1) *	0.0338(7)	0.0338(7)	0.0074(7)	0.0250(4)
Mo(2)	0.1700(5)	0.15	—	—	—	0.008(2)
	0.1801(4)	0.30	—	—	—	0.015(2)
O	0.1412(4)	1	0.040(6)	0.024(5)	0.034(4)	0.033(2)
	0.1407(6)	1	0.049(7)	0.026(5)	0.038(7)	0.038(3)
Cl	0	0.84(4)	0.021(3)	0.021(3)	0.048(6)	0.030(3)
	0	0.91(5)	0.021(2)	0.021(2)	0.048(5)	0.030(2)

*x* = 0 for all atoms; *y* = 0 for Pb, Cl and Mo; *y* = ½ for O

Values in parentheses are 1 esd

\* refined in early stages for isotropic model and then fixed. Errors refer to those obtained before fixing.

### Mo coordination and valency

As only the substructures could be refined, it was not possible to obtain meaningful Mo—O bond lengths: only 10% of the O atoms in the PbO sheet are bonded to Mo, corresponding to <1 e of scattering. No splitting of the O site was observed and no significant residual electron density was identifiable near the O atom. Furthermore, there was no indication of an apical Mo=O bond along the fourfold axis, as might be expected by analogy with the square-pyramidal coordination of  $W^{6+}$  in pinalite (Grice and Dunn, 2000). The Mo—O bond length obtained is 2.094(5) Å and the corresponding bond valence (Brese and O'Keeffe, 1991), assuming a  $Mo^{6+}$  state, is only 0.85 v.u. However, as we cannot distinguish O atoms associated with Mo—O bonds from those of Pb(2)—O bonds, it is not possible to calculate meaningful bond-valence sums for Mo in the substructure.

While microprobe analysis of synthetic parkinsonite indicates a nearly full occupancy of the Cl site, the natural crystal has a significantly reduced occupancy. Structure refinement indicates a reduced Cl occupancy for both crystals. Microprobe analysis also shows that the Mo(2) site in the natural crystal is ~50% Mo and 50% V,

but the Pb:(Mo+V) ratio is consistent with a 9:1 supercell. A comparison with komatite (Cooper and Hawthorne, 1994) suggests that  $V^{5+}$  is likely to be tetrahedrally coordinated as  $VO_4$  groups, being very different from the square-pyramidal  $MoO_5$  coordination inferred for Mo in parkinsonite (Welch *et al.* 1996). The coordination around the Mo(2) site in the substructure of the natural parkinsonite is, therefore, likely to be complex.

### Conclusion

The first structure determination of the sheet oxychloride parkinsonite has been reported here. It is confirmed that the substituent cation (Mo, V) is ordered at the Pb(2) site and avoids bonding to Cl. The Mo site, Mo(2), is located 0.5 Å from Pb at Pb(2), and is displaced along the fourfold axis. In the light of our results for parkinsonite and studies of related substituted sheet oxychlorides, all of which do not have cation vacancies, we suggest that the original formula proposed by Symes *et al.* (1994), in which cation vacancies are an integral component, is misleading. The reduced occupancy of the Pb(2) site inferred from their X-ray powder diffraction data is due to the presence of Mo, which occupies the adjacent

Mo(2) site. Consequently, the ideal stoichiometry of parkinsonite given by Symes *et al.* (1994) should be revised to  $\text{Pb}_7\text{MoO}_9\text{Cl}_2$ . The structures determined here are consistent with the presence of a significant  $\text{Pb}_9\text{MoO}_{11}\text{Cl}_2$  superstructure component identified by Welch *et al.* (1996) using electron diffraction.

## Acknowledgements

G.O.L. acknowledges support from an Erasmus Foundation studentship for his 3-month visit to the Natural History Museum, London. We thank Paola Bonazzi and Luca Bindi (Università di Firenze) for discussions of the crystal chemistry of parkinsonite and related oxychlorides. Fernando Cámara, Tony Kampf and Marco Pasero are thanked for their reviews.

## References

- Aurivillius, B. (1982) On the crystal structures of a number of non-stoichiometric mixed lead oxide halides composed of  $\text{PbO}$ -like blocks and single halogen layers. *Chemica Scripta*, **19**, 97–107.
- Blessing, R.H. (1987) Data reduction and error analysis for accurate single crystal diffraction intensities. *Crystallography Reviews*, **1**, 3–58.
- Bonaccorsi, E. and Pasero, M. (2003) Crystal structure refinement of sahlinite,  $\text{Pb}_{14}(\text{AsO}_4)_2\text{O}_9\text{Cl}_4$ . *Mineralogical Magazine*, **67**, 15–21.
- Brese, N.E. and O’Keeffe, M. (1991) Bond-valence parameters for solids. *Acta Crystallographica B*, **47**, 192–197.
- Charkin, D.O. and Lightfoot, P. (2006) Synthesis of novel lead–molybdenum and lead–tungsten oxyhalides with the pinalite structure,  $\text{Pb}_3\text{MoO}_5\text{Cl}_2$  and  $\text{Pb}_3\text{WO}_5\text{Br}_2$ . *American Mineralogist*, **91**, 1918–1921.
- Cooper, M. and Hawthorne, F.C. (1994) The crystal structure of komatite,  $\text{Pb}_{14}(\text{VO}_4)_2\text{O}_9\text{Cl}_4$ , a complex heteropolyhedral sheet mineral. *American Mineralogist*, **79**, 550–554.
- Farrugia, L.J. (1999) WinGX suite for small-molecule single-crystal crystallography. *Journal of Applied Crystallography*, **32**, 837–838.
- Grice, J.D. and Dunn, P.J. (2000) Crystal-structure determination of pinalite. *American Mineralogist*, **85**, 806–809.
- Krivovichev, S.V., Turner, R., Rumsey, M., Siidra, O.I. and Kirk, C.A. (2009) The crystal structure and chemistry of mereheadite. *Mineralogical Magazine*, **73**, 103–117.
- Rouse, R.C., Peacor, D.R., Dunn, P.J., Criddle, A.J., Stanley, C.J. and Innes, J. (1988) Asisite, a silicon-bearing lead oxychloride from the Kombat mine, South West Africa, Namibia. *American Mineralogist*, **73**, 643–650.
- Sheldrick, G.M. (2008) A short history of SHELX. *Acta Crystallographica A*, **64**, 112–122.
- Smith, G.F.H. and Prior, G.T. (1911) On schwartzembergite. *Mineralogical Magazine*, **16**, 77–83.
- Symes, R.F., Cressey, G., Criddle, A.J., Stanley, C.J., Francis, J.G. and Jones, G.C. (1994) Parkinsonite,  $(\text{Pb},\text{Mo},\square)_8\text{O}_8\text{Cl}_2$ , a new mineral from Merehead Quarry, Somerset. *Mineralogical Magazine*, **58**, 59–68.
- Welch, M.D. (2004) Pb-Si ordering in sheet-oxychloride minerals: the superstructure of asisite, nominally  $\text{Pb}_7\text{SiO}_8\text{Cl}_2$ . *Mineralogical Magazine*, **68**, 247–254.
- Welch, M.D., Schofield, P.F., Cressey, G. and Stanley, C.J. (1996) Cation ordering in lead-molybdenum-vanadium oxychlorides. *American Mineralogist*, **81**, 1350–1359.
- Welch, M.D., Cooper, M.A., Hawthorne, F.C. and Criddle, A.J. (2000) Symesite,  $\text{Pb}_{10}(\text{SO}_4)\text{O}_7\text{Cl}_4\cdot\text{H}_2\text{O}$ , a new PbO-related sheet mineral: description and crystal structure. *American Mineralogist*, **85**, 1526–1533.
- Welch, M.D., Cooper, M.A., Hawthorne, F.C. and Kyser, T.C. (2001) Trivalent iodine in the crystal structure of schwartzembergite,  $\text{Pb}_5^{2+}\text{I}^{3+}\text{O}_6\text{H}_2\text{Cl}_3$ . *The Canadian Mineralogist*, **39**, 785–795.



